*35th EPS Conference on Plasma Phys. Hersonissos, 9 - 13 June 2008 ECA Vol.**32D**, P-2.012 (2008)*

Radiation Distribution in the Full Tungsten ASDEX Upgrade

J.C. Fuchs, T. Eich, L. Giannone, A. Herrmann, W. Sandmann,

and the ASDEX Upgrade Team

Max-Planck-Institut für Plasmaphysik, EURATOM Association, Garching, Germany

Introduction

The area of tungsten coated plasma facing components (PFCs) in ASDEX Upgrade was increased continuously throughout the last years in order to investigate the plasma wall interaction and its implications in an all tungsten divertor tokamak, i.e. in absence of carbon. Finally in 2007 all PFCs have been equipped with tungsten coated graphite tiles.

The key player in order to reduce the power load on the divertor plates is the control of radiative losses. The radiation in ASDEX Upgrade discharges was routinely measured during all stages of the change onto full tungsten operation by up to 104 foil bolometers mounted in several cameras in one poloidal position around the plasma. From the measured line integrals the distribution of the radiation emissivity has been reconstructed in the divertor region as well as in the main plasma by deconvolution methods. Thanks to the comparable fast bolometer measurements of 1 ms it is also possible to resolve radiated energy losses due to type-I ELMs.

Radiation profile

The measured line integrals of all bolometers have been unfolded in order to obtain the radiation distribution in a poloidal cross section of ASDEX Upgrade. Figure 1 shows a comparison of ELM averaged radiation distributions for two similar discharges with 1 MA plasma current, about 5-6 MW additional heating power and a fractional Greenwald density of $n_e/n_{GW} \sim 0.7$. In the older discharge (left hand side) nearly all PFCs were made of carbon, whereas in the recent discharge (right hand side) all PFCs are covered with tungsten.

In the discharge with the mainly carbon wall the highest radiation densities were found in the divertor legs with values up to 7 MW/m³. The higher radiation in the inner divertor origins from ELMs, between ELMs the radiation was found to be nearly symmetrically distributed between the inner and outer divertor[1,2]. In the main plasma, the radiation distribution shows a hollow profile with emissivities up to 300 kW/m³, which cannot be seen in the chosen colour scale of figure 1. Integrating the distribution over the whole plasma volume gives a total radiated power of 3.3 MW which

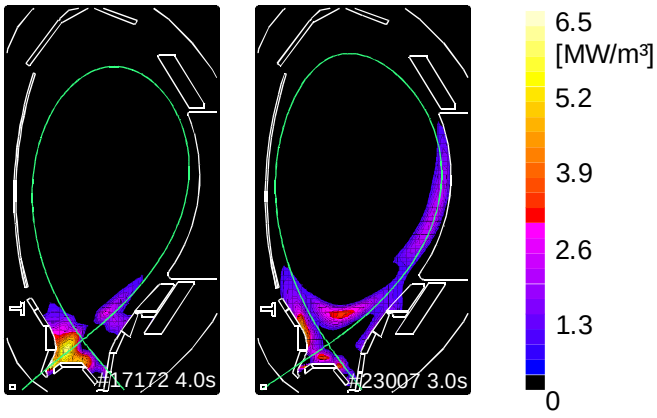

Fig. 1: Distribution of the radiation emissivity in a poloidal cross section of ASDEX Upgrade for two discharges with comparable plasma parameters. a) mostly carbon PFCs, b) full W covered PFCs

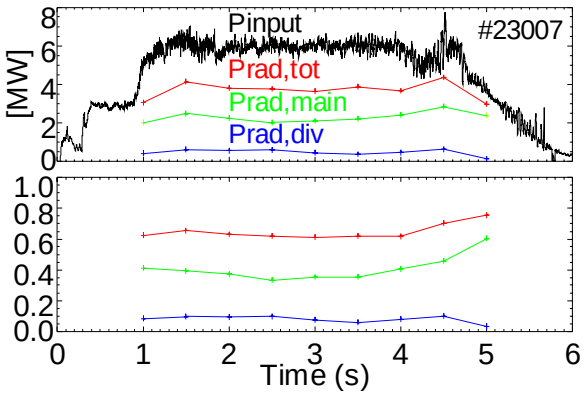

Fig. 2: Time evolution of the input power (black), total radiated power (red), radiated power in the main plasma (green) and in the divertor (blue) for the discharge from Fig. 1b. The upper picture shows absolute powers, the lower picture the fraction of the radiated power to the input power.

is about 55% of the input power. Nearly 40% of the radiated power was found in the divertor, and about 35% of the total radiated power origins in the main plasma within the last closed flux surface. The rest of the radiation was located at the plasma edge.

As long as the coverage of the PFCs with tungsten in ASDEX Upgrade was not complete, both the total radiated power and the distribution of the radiation emissivity remained more or less independent of the ratio between tungsten and carbon coated PFCs, with a slight increase of the radiation from the main plasma after increasing the tungsten coated area. After finally the last divertor tiles bearing the strike points in ASDEX Upgrade have been coated with tungsten, significant changes in the distribution of the radiation emissivity were observed. As expected, in the full tungsten device there is now clearly less radiation from the X-point and divertor region than in discharges with mixed tungsten and carbon coated PFCs, whereas the radiation from the main plasma and the edge has increased (figure 1, right hand

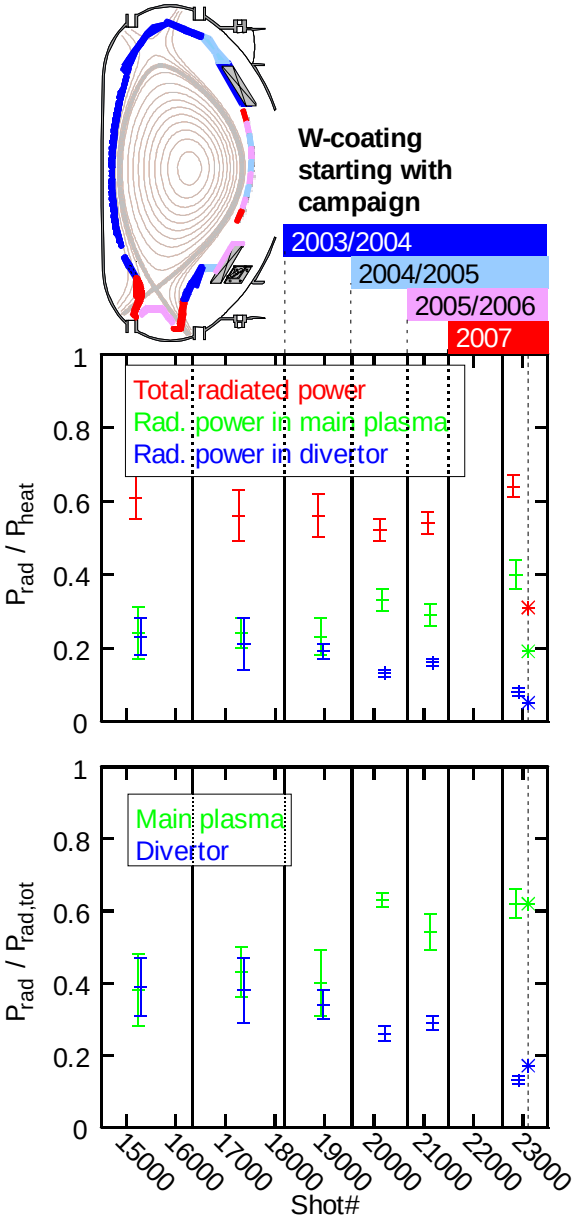

Fig. 3: Evaluation of the radiated power during the various stages of coverage of the PFCs with tungsten:The upper diagram shows the fraction of the total radiated power (red), the radiated power in the main plasma (green) and in the divertor (blue) to the input power. Plotted are mean values of comparable discharges for the campaigns of the last 7 years. The sketch above the diagrams indicates which PFCs have been covered with tungsten during the various campaigns. The lower diagram shows mean values of the fraction of the radiated power in the main plasma (green) and in the divertor (blue) to the total radiated power.
The very last points (*) in the diagrams correspond to the first discharge after the first boronization with a full tungsten wall.

side). About 60% of the input power is found as radiated power, of which only 5-10% are located in the divertor and 45% in the main plasma (figure 2).

Figure 3 shows a statistical overview of the evaluation of the radiated power during the campaigns of the past 7 years with increasing amount of tungsten covered PFCs. For each campaign the mean values from discharges with similar plasma parameters to those from the discharges in figure 1 are plotted. Due to technical problems no bolometer data from the horizontal camera were available in the 2007 campaign. It can be seen that in the full tungsten tokamak the radiation from the divertor has decreased, whereas the radiation from the main plasmas has increased as discussed earlier exemplary with the two discharges from figure 1.

Whereas the discharges from previous campaigns were performed with more or less boronized wall conditions, the shots in the last campaign with a pure tungsten wall (up to the dashed line) were without any boronization. The very last point in figure 3 corresponds to the first shot after the first boronization in the full tungsten device, it shows a clearly reduced radiated power, where the distribution of the radiation between divertor and main plasma remains unchanged. This behaviour was already observed earlier after boronizations in a mixed tungsten and carbon machine, and it is expected that the radiation increases to its 'normal' lever again after some ten discharges.

Power balance

Figure 4 shows the power balance for the discharge from figure 1b in a full tungsten tokamak: Subtracting the total radiated power measured by bolometers, the power load on the divertor tiles measured by IR-cameras, and the change of the MHD energy of the plasma from the input power and taking into account that parts of the divertor radiation are recorded by both bolometers and thermographic cameras, a remaining part of 20% of the input power is left, which is similar to the value found at JET[3]. This remaining power may be explained by power load on tiles in the midplane and also partly in the divertor which are not observed by thermographic cameras. A hint that the power load onto divertor tiles might be higher than measured by the thermographic cameras is that the accumulated energy on these tiles measured by calorimetry is higher than the integrated power load measured by thermography.

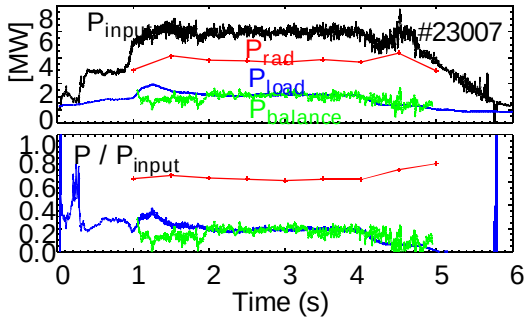

Fig. 4: Power balance for the discharge from figure 1b: Input power (black), total radiated power (red), power load to divertor tiles (blue) and power balance (green, see text) as absolute values (top) and as fractions to the input power (bottom)

Central radiation peaking

Although the radiation in the main plasma origins mostly from the plasma edge, in some conditions, especially with high temperature edge plasmas close to the ICRH antennas when in operation, a strong increase of the central radiation in line with central peaking of the tungsten

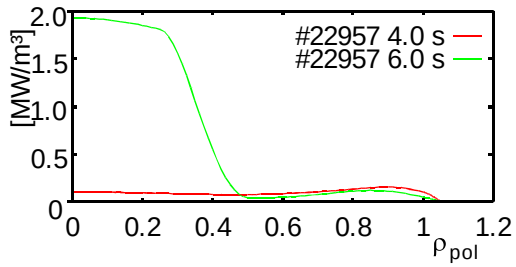

Fig. 5: Radiation profile in the main plasma as a function of the normalized flux radius during phases without ECRH heating (green) and with ECRH heating (red). The central radiation was kept successfully low by applying ECRH.

concentration was observed. This central peaking was kept successfully low by use of ECRH heating instead[4]. Figure 5 shows a comparison between two radiation profiles in the main plasma, one during a phase with ECRH heating, showing a normal hollow profile, the second after ECRH has been switched off with a strong central radiation peaking. Although the highest radiation densities are still near the divertor, due to the larger radiating volume in the centre the radiation from the main plasma has increased to 80% of the total radiated power.

Radiation during type-I ELMs

By using the accumulated energy on a bolometer foil instead of the momentarily absorbed power it is possible to investigate the radiation energy losses due to type-I ELMs[2]. In order to minimize noise in the bolometric measurements, newly built amplifiers[5] for the main horizontal bolometer camera have been equipped with bandwidth filters which however reduce the effective time resolution. Therefore, no reconstruction of the radiation distribution during ELMs could be done for discharges from the recent tungsten campaign. Since the main vertical camera still has the full time resolution of 1 ms, it is possible to get an estimate for the total radiated energy during and between type-I ELMs by summing up the geometry of these lines of sight through the plasma. Due to the difficult coverage of some divertor volumes this value may be underestimated by about 15%, similar to the effect described at JET[6].

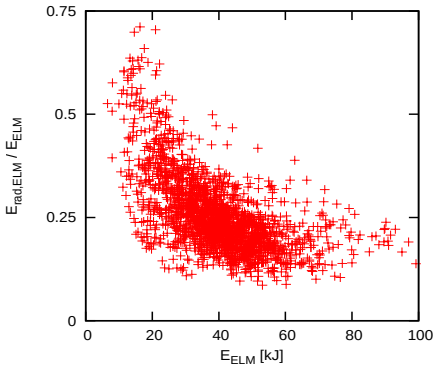

Fig. 6: Distribution of the normalized radiated energy due to an type-I ELM $\Delta E_{rad,ELM}/E_{ELM}$ as a function of the ELM energy.

Figure 6 shows for a number of type-ELMs from discharges with a pure tungsten wall the dependence of the normalized ELM radiation $\Delta E_{rad,ELM}/E_{ELM}$ on the ELM energy E_{ELM}. Typically about 25% of the ELM energy are found as radiation, whereas in a carbon machine a value of 40% was found [2]. A more detailed analysis of the radiation during ELMs is in progress.

References

[1] A. Kallenbach et.al., Nuclear Fusion **39** (1999), 901-917
[2] J.C. Fuchs et.al., Journal of Nuclear Materials **337-339** (2005) 756-760
[3] T. Eich et.al., Plasma Phys. Control. Fusion **49** (2007) 573-604
[4] R. Neu et.al., Plasma Phys. Control. Fusion **49** (2007) B59–B70
[5] L. Giannone et.al., Plasma Phys. Control. Fusion **47** (2005) 2123–2143
[6] L.C. Ingesson (1999), Report JET-R(99)06